

WIND NOISE SIMULATION OF THE A-PILLAR AND SIDE VIEW MIRROR  
USING GENERIC VEHICLE MODEL, DrivAer

NUR HAZIQAH BINTI SHAHARUDDIN

A thesis submitted in fulfilment of the  
requirements for the award of the degree of  
Master of Philosophy

Malaysia-Japan International Institute of Technology  
Universiti Teknologi Malaysia

SEPTEMBER 2022

## DEDICATION

*This thesis is dedicated to*

*My beloved mother*

*My beloved father*

*My special youngest brother*

*Family members*

*That always make my life so meaningful and cheerful because of their love*

*This thesis also is dedicated to*

*a very responsible, kind-hearted, charming,*

*young talented manager*

*Tharveen a/l Puroshuman*

## ACKNOWLEDGEMENT

It would not have been possible to complete this project without the kind support and help of many individuals and organizations. I would like to extend my sincere thanks to all of them. First and foremost, I would like to express the deepest appreciation to my supervisor, Associate Prof Dr. Mohamed Sukri Mat Ali, for his patience, guidance, knowledge and constant supervision as well as providing necessary information on this project and also have given much support and help in completing this thesis.

My special gratitude also expressed to my parents and family members for their support and prayers. They have given a lot of encouragement to me to get along with all the difficulties in completing this thesis. They are the stronger supporters after all. They have given me much inspiration and they are the reason for me to keep facing all the struggles, pain and hardships until this time.

Next, special thanks to all of the members of Wind Engineering for (Urban, Artificial, Man-made) Environment (WEE) laboratory that have given much help by teaching me about many things related to this project and also for their kind cooperation, support and advice.

Last but not least, special thanks also for the UTM Guards and *Makcik* cleaners at the MJIT Level 1 and Level 10 and most special thanks to the managers and team members of Pizza Hut Gurney Mall UTMKL for their support since October 2019 until July 2022.

## ABSTRACT

Vehicle interior noise level has now become one of the indicators of driving comfort. However, the generation of noise is a complex phenomenon where it involves various sound sources with different ways of radiation. This research focuses on the generation of wind noise from the A-pillar and side-view mirror of a generic vehicle model known as DrivAer, based on the physical flow behaviour. The main objective of this study is to find the physical flow that causes the generation of A-pillar wind noise and to propose the relation between the A-pillar angles and length of side-view mirror with wind noise generation. This study is conducted numerically at a Reynolds number of  $Re = 12.17 \times 10^6$ , with respect to the length of DrivAer model. The noise source is obtained from the incompressible Unsteady Reynolds Averaged Navier-Stokes (URANS); and the noise radiation is predicted using an acoustic analogy based on Curle's equations. Reliability and validity of the calculations are tested by comparing the basic model with data of experimental studies from previous researchers, whereby the result indicates an almost similar outcome. A total of eight main cases have been studied. These cases include A-pillar cases of varying angles which are  $61^\circ$ ,  $58^\circ$  (baseline case),  $50^\circ$  and  $42^\circ$ ; and four side view mirror cases of varying gaps which are 180mm, 190mm, 230mm and 240mm. Results have shown that increasing the A-pillar angle makes the sound pressure level louder. 84.33 dB is generated when the A-pillar angle is at  $61^\circ$  and 76.41 dB is generated when the A-pillar angle is at  $42^\circ$ . The formation of the A-pillar conical vortex formed along the A-pillar has been found responsible for the generation of the wind noise. In the case of different side-view mirror position, in which the A-pillar angle remains constant, results for all cases are almost the same according to the A-pillar sound pressure level and sound source level results, in which the noise generated is about 82 dB for all cases of side-view mirror.

## ABSTRAK

Tahap kebisingan dalaman sesebuah kenderaan kini menjadi salah satu petunjuk terhadap keselesaan pemanduan. Walau bagaimanapun, penghasilan kebisingan merupakan fenomena yang kompleks di mana penghasilannya melibatkan pelbagai sumber bunyi dengan cara radiasi yang berbeza. Penyelidikan ini menumpukan kepada penjanaan kebisingan daripada A-pillar dan cermin sisi kenderaan generik yang dikenali sebagai DrivAer, berdasarkan kelakuan fizikal aliran angin yang melepaskannya. Objektif utama penyelidikan ini adalah untuk mengenal pasti aliran fizikal yang bertanggungjawab kepada penjanaan kebisingan daripada A-pillar dan cermin sisi kenderaan, dan juga untuk menghubungkan kaitkan antara sudut A-pillar dan kepanjangan cermin sisi dalam penghasilan kebisingan angin. Kajian ini telah dijalankan secara numerial pada nombor Reynolds  $Re = 12.17 \times 10^6$ , berdasarkan kepada panjang model DrivAer dengan menggunakan persamaan *Unsteady Reynolds Averaged Navier-Stokes* (URANS) dan pengiraan kebisingan telah dilakukan dengan menggunakan teori Curle. Data kajian daripada model dasar telah dibandingkan dengan data kajian eksperimen yang telah dijalankan oleh penyelidik terdahulu untuk tujuan pengesahan dan kebolehpercayaan pengiraan. Data kajian telah menunjukkan hasil yang hampir sama seperti eksperimen yang telah dijalankan penyelidik terdahulu. Terdapat lapan jumlah keseluruhan kes yang dijalankan dalam kajian ini. Kes-kes tersebut adalah kes A-pillar dengan sudut yang berbeza iaitu  $61^\circ$ ,  $58^\circ$  (model dasar),  $50^\circ$  and  $42^\circ$  dan juga empat kes yang melibatkan cermin sisi yang berlainan panjang iaitu 180mm, 190mm, 230mm and 240mm. Hasil kajian mendapati bahawa semakin landai sudut A-pillar, semakin tinggi tahap kebisingan yang dihasilkan. 84.33dB tahap kebisingan telah dihasilkan oleh sudut A-pillar  $61^\circ$  dan 76.41dB dihasilkan daripada sudut A-pillar  $42^\circ$ . Kajian juga mendapati bahawa pembentukan konikal vorteks A-pillar sepanjang A-pillar memainkan peranan dalam penghasilan kebisingan angin. Bagi kes cermin sisi yang berbeza panjang pula, di mana sudut A-pillar ditetapkan pada sudut yang sama, hasil kajian mendapati kesemua kes menghasilkan tahap kebisingan yang hampir sama, di mana tahap kebisingan yang terhasil adalah dalam lingkungan 82 dB.

## TABLE OF CONTENTS

|                  | <b>TITLE</b>  | <b>PAGE</b>  |
|------------------|---|--------------|
|                  | <b>DECLARATION</b>                                    | <b>iii</b>   |
|                  | <b>DEDICATION</b>                                     | <b>iv</b>    |
|                  | <b>ACKNOWLEDGEMENT</b>                                | <b>v</b>     |
|                  | <b>ABSTRACT</b>                                       | <b>vi</b>    |
|                  | <b>ABSTRAK</b>  | <b>vii</b>   |
|                  | <b>TABLE OF CONTENTS</b>                              | <b>viii</b>  |
|                  | <b>LIST OF TABLES</b>                                 | <b>xi</b>    |
|                  | <b>LIST OF FIGURES</b>                                | <b>xii</b>   |
|                  | <b>LIST OF ABBREVIATIONS</b>                          | <b>xvi</b>   |
|                  | <b>LIST OF SYMBOLS</b>                                | <b>xvii</b>  |
|                  | <b>LIST OF APPENDICES</b>                             | <b>xviii</b> |
| <b>CHAPTER 1</b> | <b>INTRODUCTION</b>                                   | <b>1</b>     |
|                  | 1.1 Research Background                               | 1            |
|                  | 1.2 Problem Statement                                 | 6            |
|                  | 1.3 Research Objective                                | 7            |
|                  | 1.4 Research Scope and Limitations                    | 7            |
|                  | 1.5 Significance of Research                          | 9            |
|                  | 1.6 Thesis Outline                                    | 10           |
| <b>CHAPTER 2</b> | <b>LITERATURE REVIEW</b>                              | <b>11</b>    |
|                  | 2.1 Overview on Aerodynamic Flow over Bluff Body      | 11           |
|                  | 2.2 Noise Generation Mechanisms in Passenger Car      | 13           |
|                  | 2.3 Wind Noise from the A-pillar and Side View Mirror | 15           |
|                  | 2.4 Chapter Summary and Research Gap                  | 34           |
| <b>CHAPTER 3</b> | <b>RESEARCH METHODOLOGY</b>                           | <b>35</b>    |
|                  | 3.1 Flow Simulation (Near-field simulation)           | 35           |

|                  |   |           |
|------------------|---|-----------|
| 3.1.1            | Governing Equations   | 36        |
| 3.1.2            | Turbulence Model  | 37        |
| 3.1.3            | Wall Function   | 39        |
| 3.1.4            | Problem Geometry  | 41        |
| 3.1.5            | Computational Domain and Boundary Conditions                          | 43        |
| 3.1.6            | Computing Machine   | 44        |
| 3.2              | Noise Simulation (Far-field simulation)                               | 45        |
| 3.2.1            | Acoustic Analogy  | 45        |
| 3.2.2            | Lighthill's Theory  | 47        |
| 3.2.3            | Curle's Theory  | 50        |
| 3.2.4            | Noise Calculation from the A-pillar                                   | 54        |
| 3.2.5            | Noise Calculation from the Side View Mirror                           | 57        |
| 3.3              | Research Flow Chart   | 58        |
| 3.4              | Chapter Summary   | 59        |
| <b>CHAPTER 4</b> | <b>COMPARISON AND VALIDATION STUDY</b>                                | <b>60</b> |
| 4.1              | Flow Validation   | 60        |
| 4.1.1            | Grid Refinement Study   | 61        |
| 4.1.1.1          | Mesh Description  | 61        |
| 4.1.2            | Results from Grid Refinement Study                                    | 63        |
| 4.1.2.1          | Richardson Extrapolation  | 64        |
| 4.1.2.2          | Grid Convergence Index  | 65        |
| 4.1.2.3          | Forces coefficient and Turbulence Model                               | 70        |
| 4.1.2.4          | Flow Visualisation  | 72        |
| 4.1.2.5          | Pressure Coefficient  | 74        |
| 4.2              | Noise Validation  | 76        |
| 4.2.1            | Boundary Condition Settings   | 77        |
| 4.2.2            | Analogy of Noise Calculation using Curle's Theory                     | 79        |
| 4.2.3            | Comparison Results of Sound Pressure Level (SPL) for SAE Type 4 model | 81        |
| 4.3              | Chapter Summary   | 82        |

|                             |  |            |
|-----------------------------|--|------------|
| <b>CHAPTER 5</b>            | <b>RESULTS AND DISCUSSIONS</b>                                     | <b>83</b>  |
| 5.1                         | Background of Study  | 83         |
| 5.2                         | Noise from Different Angle of A-pillar                             | 87         |
| 5.2.1                       | Noise from A-pillar  | 88         |
| 5.2.1.1                     | Noise Characteristics from A-pillar                                | 88         |
| 5.2.1.2                     | Aerodynamics Behaviour   | 92         |
| 5.2.2                       | Noise from side view mirror  | 95         |
| 5.2.2.1                     | Aerodynamics Behaviour   | 95         |
| 5.2.2.2                     | Noise Characteristics from Side View Mirror                        | 96         |
| 5.2.3                       | Total Noise from Different Angle of A-pillar and Side View Mirror  | 98         |
| 5.2.3.1                     | Flow Visualisations  | 101        |
| 5.3                         | Noise from Different Length of Side View Mirror                    | 104        |
| 5.3.1                       | Noise from A-pillar  | 105        |
| 5.3.1.1                     | Noise Characteristics from A-pillar                                | 105        |
| 5.3.1.2                     | Aerodynamics Behaviour   | 108        |
| 5.3.2                       | Noise from Side View Mirror  | 110        |
| 5.3.2.1                     | Aerodynamics Behaviour   | 110        |
| 5.3.2.2                     | Noise Characteristics from Side View Mirror                        | 112        |
| 5.3.3                       | Total Noise from A-pillar and Different Length of Side View Mirror | 114        |
| 5.3.3.1                     | Flow Visualisation   | 115        |
| 5.4                         | Chapter Summary  | 118        |
| <b>CHAPTER 6</b>            |  | <b>120</b> |
| 6.1                         | Research Outcome   | 120        |
| 6.2                         | Future Works   | 121        |
| <b>REFERENCES</b>           |  | <b>123</b> |
| <b>LIST OF PUBLICATIONS</b> |  | <b>133</b> |



## LIST OF TABLES

| TABLE NO. | TITLE  | PAGE |
|-----------|--|------|
| Table 1.1 | Standard European vehicles measurement regulations [18, 19, 20]  | 8    |
| Table 3.1 | Numerical boundary conditions setting in OpenFOAM  | 44   |
| Table 3.2 | Numerical boundary conditions setting in OpenFOAM  | 45   |
| Table 4.1 | Parameters used for all cases  | 62   |
| Table 4.2 | Comparison of forces coefficient parameter between the three mesh resolutions and the extrapolated value based on Richardson Extrapolation calculation | 67   |
| Table 4.3 | Order of accuracy and Grid Convergence Index for three grid resolution based on forces coefficient parameter   | 68   |
| Table 4.4 | The $y^+$ values on the wall for all cases   | 71   |
| Table 4.5 | Comparison of drag coefficient ( $C_D$ ) between current study and previous studies  | 72   |
| Table 4.6 | Dimension of SAE Type 4 model  | 77   |
| Table 4.7 | Numerical boundary conditions for SAE Type 4   | 79   |
| Table 4.8 | Solver setting used in OpenFOAM for SAE Type 4   | 79   |
| Table 5.1 | Total number of cases involved in this study   | 84   |
| Table 5.2 | Number of mesh for each case   | 86   |
| Table 5.3 | Drag and Lift coefficient for different angle of A-pillar cases  | 93   |
| Table 5.4 | Aerodynamic forces acting on the side view mirror  | 95   |
| Table 5.5 | Aerodynamic forces coefficient acting on the side view mirror  | 111  |
| Table 5.6 | Sound pressure level for the case of different angle of A-pillar   | 119  |
| Table 5.7 | Sound pressure level for the case of different length of side view mirror  | 119  |

## LIST OF FIGURES

| <b>FIGURE NO.</b> | <b>TITLE</b>   | <b>PAGE</b> |
|-------------------|--|-------------|
| Figure 1.1        | Noise level based on different situations  | 2           |
| Figure 1.2        | Relationship between the speed of car and the sound power level for each noise sources [7]                     | 3           |
| Figure 1.3        | Three pillar configurations of DrivAer Fastback, a sedan-typed car model                                       | 6           |
| Figure 2.1        | Viscous flow around circular cylinder (taken from White [30])  | 12          |
| Figure 2.2        | Schematic representation of flow pattern over a passenger car (taken from Katz [38])                           | 14          |
| Figure 2.3        | Schematic representation of A-pillar vortex (taken from Katz [38])   | 15          |
| Figure 2.4        | Conical vortex flow structure around the A-pillar [44]   | 16          |
| Figure 2.5        | Pressure distribution around the A-pillar of a simple car model [44]   | 17          |
| Figure 2.6        | Comparison of surface pressure fluctuation for three different car design [33]                                 | 18          |
| Figure 2.7        | Streamlines for three different angle of A-pillar [50]   | 20          |
| Figure 2.8        | Comparison of PFL at the A-pillar [6]  | 21          |
| Figure 2.9        | Pressure fluctuations at the A-pillar and side window [21]   | 24          |
| Figure 2.10       | Pressure distribution on side window based on different length of side view mirror [21]                        | 25          |
| Figure 2.11       | Streamline results for airflow passing through A-pillar and side view mirror                                   | 27          |
| Figure 2.12       | Streamline results based on vorticity magnitude. Side window mounted (top) and Door mounted (bottom)           | 29          |
| Figure 2.13       | Isosurfaces of Q-criterion for LES (top) and DDES (bottom)   | 31          |
| Figure 2.14       | Frequency spectra at the wake of the side mirror model (a) URANS (b) DDES (c) LES                              | 32          |
| Figure 2.15       | Results of pressure fluctuation (top) and mean velocity (bottom) for (a) narrow A-pillar and (b) wide A-pillar | 33          |

|             |  |    |
|-------------|--|----|
| Figure 3.1  | Wall function of different layer   | 41 |
| Figure 3.2  | The DrivAer model provided by TUM with three different rear end and two different underbody [24]                                       | 42 |
| Figure 3.3  | Dimension of DrivAer Fastback model [75]   | 42 |
| Figure 3.4  | Computational domain for DrivAer model for flow simulations  | 43 |
| Figure 3.5  | Directivity pattern for three different types of noise sources. (a) Monopole (b) Dipole (c) Quadrupole                                 | 46 |
| Figure 3.6  | Points along the DrivAer Fastback A-Pillar   | 54 |
| Figure 3.7  | Directivity pattern of a dipole (left) and directivity of noise to observer (right)  | 56 |
| Figure 3.8  | DrivAer Fastback Side View Mirror  | 57 |
| Figure 3.9  | Research flow chart of study   | 59 |
| Figure 4.1  | Side view for mesh generation of all cases. (a) Coarse (b) Medium (c) Fine   | 62 |
| Figure 4.2  | Front view for mesh generation of all cases. (a) Coarse (b) Medium (c) Fine  | 63 |
| Figure 4.3  | Extrapolated value of $CD_{mean}$  | 68 |
| Figure 4.4  | Percentage error for $CD_{mean}$   | 69 |
| Figure 4.5  | Extrapolated value of $CL_{mean}$  | 70 |
| Figure 4.6  | Percentage error for $CL_{mean}$   | 70 |
| Figure 4.7  | Distribution of $y^+(yPlus)$ on the DrivAer Fastback model   | 71 |
| Figure 4.8  | Iso-surface of the second invariant (Q) based on mean velocity magnitude. Current study (top), study by Ruttgers et al. (bottom) [98]. | 73 |
| Figure 4.9  | Streamlines at the symmetry of the model. Current study (Top), Study by Guilmineau (Bottom) [95]                                       | 74 |
| Figure 4.10 | Pressure coefficient ( $C_p$ ) distribution on top of DrivAer Fastback model at the symmetry plane                                     | 75 |
| Figure 4.11 | Pressure coefficient ( $C_p$ ) distribution below of DrivAer Fastback model at the symmetry plane                                      | 76 |
| Figure 4.12 | Simplified vehicle model, SAE Type 4 (fullback)  | 77 |
| Figure 4.13 | Computational domain for SAE Type 4 model. (a) Side view (b) Front view  | 78 |

|             |  |     |
|-------------|--|-----|
| Figure 4.14 | Sound Pressure Level (SPL)   | 80  |
| Figure 4.15 | Sound Pressure Level (SPL) results of study by Hartmann et. al [14] (experiment and simulations) and current study | 81  |
| Figure 5.1  | Angle of A-pillar is measured vertically from the A-pillar (side view)   | 84  |
| Figure 5.2  | Length of side view mirror manipulated at <i>y-axis</i> position (Top view)  | 85  |
| Figure 5.3  | Figure (a) (c) and (d) is the model that has been modified from the original (baseline) model                      | 85  |
| Figure 5.4  | Modified model for side view mirror cases  | 86  |
| Figure 5.5  | Probes location selected around the A-pillar and the observer position   | 87  |
| Figure 5.6  | Sound source level on each A-pillar small element  | 89  |
| Figure 5.7  | Sound pressure fluctuations of the A-pillar for all cases  | 90  |
| Figure 5.8  | Sound pressure level along the A-pillar measured at the observer position  | 91  |
| Figure 5.9  | Distribution of power spectrum density (PSD) of different angle of A-pillar  | 92  |
| Figure 5.10 | Surface pressure coefficient distributions along the A-pillar of all cases.  | 93  |
| Figure 5.11 | Surface mean pressure at the A-pillar of all cases   | 94  |
| Figure 5.12 | Resultant of fluctuating forces acting on the side view mirror   | 96  |
| Figure 5.13 | Sound pressure fluctuations from the side view mirror at four different angle of A-pillar case                     | 97  |
| Figure 5.14 | Power spectrum density of noise from side view mirror for different angle of A-pillar cases                        | 98  |
| Figure 5.15 | Total sound pressure distribution for all cases of different angle of A-pillar                                     | 99  |
| Figure 5.16 | Total power spectrum density of all cases.   | 100 |
| Figure 5.17 | Vorticity behaviour around the A-pillar coloured by mean velocity  | 102 |
| Figure 5.18 | Vorticity behaviour around the side view mirror coloured by mean velocity  | 104 |
| Figure 5.19 | Sound source level along the A-pillar for all side view mirror cases.  | 106 |

|             |  |     |
|-------------|--|-----|
| Figure 5.20 | Total sound pressure fluctuations from points selected along the A-pillar                | 106 |
| Figure 5.21 | Sound pressure level from the A-pillar   | 107 |
| Figure 5.22 | Power spectrum density of A-pillar   | 108 |
| Figure 5.23 | Pressure coefficient along the A-pillar for different side view mirror case              | 109 |
| Figure 5.24 | Surface mean pressure along the A-pillar   | 110 |
| Figure 5.25 | Resultant force coefficient  | 112 |
| Figure 5.26 | Sound pressure fluctuations for different length of side view mirror cases               | 113 |
| Figure 5.27 | Sound spectrum distribution for different length of side view mirror cases               | 114 |
| Figure 5.28 | Total sound pressure distribution from A-pillar and different length of side view mirror | 115 |
| Figure 5.29 | Total power spectrum density   | 115 |
| Figure 5.30 | Vorticity behaviour around the A-pillar coloured by mean velocity                        | 117 |
| Figure 5.31 | Vorticity behaviour around the side view mirror coloured by mean velocity                | 118 |

## LIST OF ABBREVIATIONS

|       |   |  |
|-------|---|--|
| CFD   | - | Computational Fluid Dynamics             |
| DES   | - | Detached Eddy Simulation                 |
| DDES  | - | Delayed Detached Eddy Simulation         |
| LES   | - | Large Eddy Simulation                    |
| URANS | - | Unsteady Reynolds Averaged Navier-Stokes |
| DNS   | - | Direct Numerical Simulation              |
| TUM   | - | Technology University of Munchen         |
| SVM   | - | Side View Mirror                         |
| SPL   | - | Sound Pressure Level                     |
| SSL   | - | Sound Source Level                       |
| SEA   | - | Statistical Energy Analysis              |
| LBM   | - | Lattice Boltzmann method                 |
| SST   | - | Shear Stress Transport                   |
| PSD   | - | Power Spectrum Density                   |

## LIST OF SYMBOLS

|              |   |                                    |
|--------------|---|------------------------------------|
| dB           | - | Decibels                           |
| Hz           | - | Hertz                              |
| A            | - | Characteristics area of bluff body |
| L            | - | Length, Lift force                 |
| D            | - | Drag force                         |
| W            | - | Width                              |
| H            | - | Height                             |
| R            | - | Distance of observer               |
| $U_{\infty}$ | - | Upstream velocity                  |
| F            | - | Force                              |
| $u$          | - | Velocity                           |
| p            | - | Pressure                           |
| St           | - | Strouhal number                    |
| $\lambda$    | - | Wavelength                         |
| Re           | - | Reynolds Number                    |
| x            | - | Streamwise direction               |
| y            | - | Crosswise direction                |
| z            | - | Spanwise direction                 |
| $\nu$        | - | Kinematic viscosity of fluid       |
| $f$          | - | Frequency                          |
| $C_o$        | - | Speed of sound                     |

## LIST OF APPENDICES

| <b>APPENDIX</b> | <b>TITLE</b> | <b>PAGE</b> |
|-----------------|--------------|-------------|
| Appendix A      | Matlab code  | 131         |



# CHAPTER 1

## INTRODUCTION

### 1.1 Research Background

According to a fact, a healthy human ear is capable of hearing sounds with frequencies in the range of 20 Hz to 20 000 Hz. Nevertheless, the ability to hear sounds at higher frequency range declines with age. The frequencies above 20 000 Hz or 20 kHz is called as ultrasonic sound and it is inaudible to a human being. Meanwhile sounds lower than 20 Hz is known as the infrasonic sound, in which it cannot be heard, but can be felt only if it is sufficiently strong. Sound may be pleasant or unpleasant, in which unpleasant sound will be called as noise [1].

Noise that is known to cause annoyance, may lead to hearing impairment and may interfere communications. Nowadays, similar to the air and water pollutions, noise also has been recognised as a major environmental pollution. Rapid industrialisation of motorisation and aviation has clearly resulted in the rapid increases of noise pollution and it becomes of significant important. Not missed, Malaysia also always looking forward for a better way in reducing the nuisance from all possible noise sources. It was reported in *The Star*, a total of 132 complaints were lodged with the Environment Department (DOE) in 2015 about the noise pollution that comes from many sources such as construction, use of roads, railways and airports [2].

Basically, the noise level perceived by humans is depending on the surrounding possible noise sources as shown in Figure 1.1. Road traffic is the most common noise pollution source because it is the most pervasive, where their noise levels could achieved about 90 to 120 dB depends on the heaviness of the traffic. A survey on noise environment in Roorkee, India, conducted by Rajeev [3] also has found that 87 percent of the community from various ages are affected by the noise emanating from the automobiles.

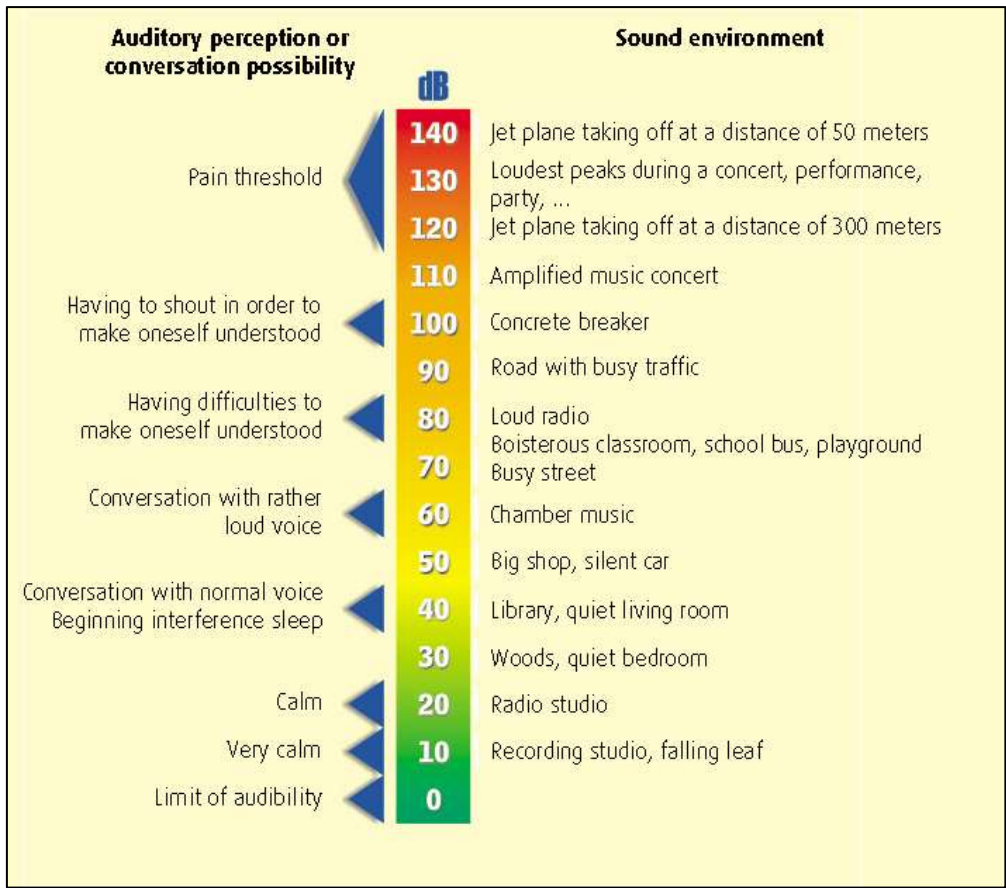


Figure 1.1 Noise level based on different situations

When it comes about the road traffic, passenger cars are seem to be one of the road vehicle that contributes significantly to the noise pollution. This is due to the number of passenger cars that outnumbers the other road vehicles especially at high speeds. One of the noise sources generated by passenger car is the aerodynamic noise. Aerodynamic noise is the mechanism of production of noise that arises almost entirely from the airflow instabilities. For moving vehicles, this is also known as the wind noise. The generation of wind noise is one of the crucial problem. Examples include the wind noise emitted from flow passes over pantograph system of high speed train when its speed exceeds 320km/h and the landing gear system of an aircraft. Also, the radiated noise from the aircraft undercarriage is one of the dominant noise source when an aircraft is in the final approach for landing [4, 5].

Deeply focusing on the passenger car problems, the noise emitted from a moving car is a total contribution mainly from three major noise sources. They are

from the engine (propulsion noise), tyre (rolling noise) and turbulent flow (wind noise). While cruising at high speed, mostly over 80km/h, the wind noise will dominates the total contribution of noise while the other two noise sources reduced significantly [6]. This is due to the fact that the wind noise increases as the speed of car increases. The increase in wind noise is proportional to the order of  $v^6$ , while the other two noise sources are proportional to the order of  $v^1$  to  $v^3$ . Here,  $v$  is the cruising speed of the cars. Figure 1.2 clearly explains the situation based on the relationship between the speed of cars and its sound power level.

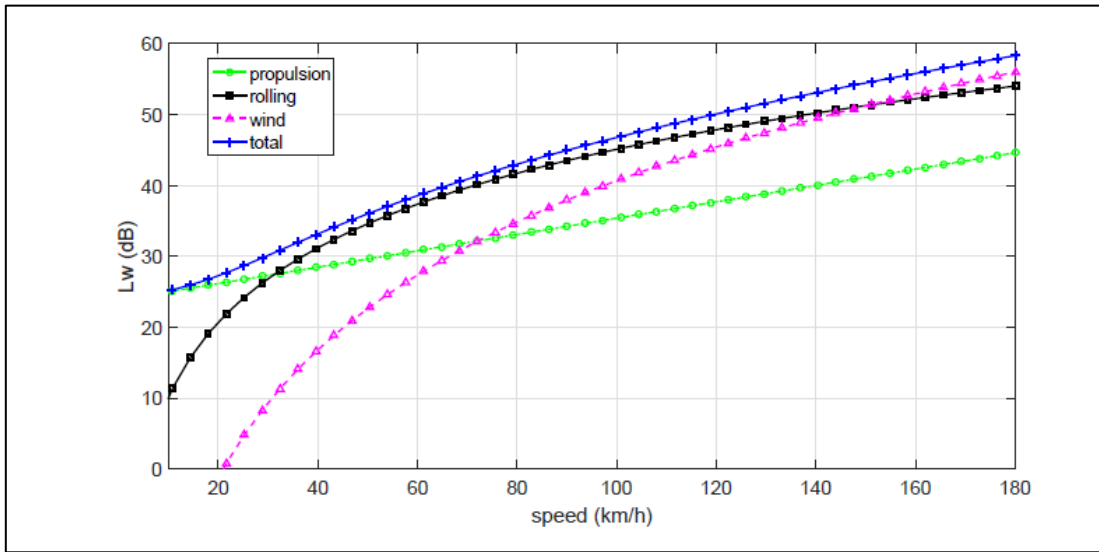


Figure 1.2 Relationship between the speed of car and the sound power level for each noise sources [7]

Theoretically, the change in sound power level with respect to the speed of the car for all type of noise sources can be estimated as follows [8, 9];

$$L_{w_{propulsion}}(v, a) = A_{propulsion} + B_{propulsion} \left( \frac{v - v_{ref}}{v_{ref}} \right) + C_{propulsion} \cdot a \quad (1.1)$$

$$L_{w_{rolling}}(v) = A_{rolling} + B_{rolling} \cdot \log_{10} \left( \frac{v}{v_{ref}} \right) \quad (1.2)$$

$$L_{w_{aero}}(v) = 10 \log_{10} \left[ \frac{A_{aero} \left( \frac{v^n}{c_0^{n-3}} \right)}{1 \times 10^{-12}} \right] \quad (1.3)$$

Here  $A, B$  and  $C$  are constant. Those constant values are governed by the condition of the road, type of car and geometry. In the Equation (1.1) to Equation (1.3),  $a$  is the acceleration of the car,  $c_0$  is the speed of sound and  $n$  is the type of wind sources. The type of wind sources are varied between the ranges of 4 to 8 that indicates the power level of sound. According to Lighthill [10]  $n = 4$  indicates as monopole type of wind sources,  $n = 6$  for dipole and  $n = 8$  for quadrupole type of wind sources.

In a long driving trip, continuous exposure to wind noise can cause fatigue and discomfort to the vehicle occupants especially the driver. The characteristic of the wind noise of a passenger car depends on several factors. They are the shape of the car, its cruising speed, wind direction flow towards the car and the natural wind condition. Among all of those factors, the shape of the car is the most important and seen as the only controllable factor for the wind noise. Since 1921, car manufacturers have given a much focus on the design of the car to be more attractive and its aerodynamic performance in order to reduce the fuel consumption. However, on late 1960s, as the car's speed has progressively increased in line with high aerodynamic performance, researchers and engineers become aware that the wind noise is increasing with the speed. This is due to the wake generated around the exterior car component such as the A-pillar and the side view mirror. When the airflow passed around the A-pillar and the side view mirror, vortex is generated and the pressure fluctuations from the vortex shedding generate wind noise. Hucho [11] stated that when a car moving at 150 km/h with 5500 rpm engine speed, 78.5 dB from the total noise of 85 dB that are measured at the driver's ear, is generated by the wind noise. Therefore, it is important to control the generated wind noise in order to reduce the total noise generated by the car.

Studies of noise generation are particularly important for passenger comfort and also for reducing the environmental noise pollution. As passenger comfort becomes increasingly important, noise reduction has to be considered in the early

design process and need to be investigated numerically in the early design stage to avoid a poor design choices [6, 12]. Therefore, it is important to have a better understanding on the wind noise generation on a passenger car so that a practical method can be applied to reduce the noise being generated.

Recently, general investigations of the flow field around the A-pillar and side view mirror are strongly focused on simplified car models, such as the Ahmed body [13] and the SAE model [14]. Both models provide a better understanding on identifying and analysing the basic flow structures by reducing the interference effects between different areas of vehicles. Previous works based on the simplified models have provide many information on numerical and experimental that is suitable for the validation purposes for further study. However, the shape of this car is no longer relevant to the current car design, where a more aerodynamic shape is more prominent. In order to close this gap, the Institute of Aerodynamics and Fluid Mechanics of the Technical University Munchen (TUM), in cooperation with Audi AG and BMW Group have proposed a realistic generic car model, which is called the DrivAer [15].

DrivAer body is a general vehicle model that is purposely designed to have a similar exterior design feature to most production cars. The geometry which is made available to the public by TUM, has been used in many studies previously as a benchmark case. Thus, the DrivAer model will be used in this study as it reflects to a realistic production car. Many studies on DrivAer for the exterior aerodynamics have been done previously, but the study on the wind noise from the A-pillar and side view mirror of DrivAer is still not yet available. DrivAer, a sedan-typed car, is divided into three pillar that is known as the A, B and C pillar as shown in Figure 1.3. Therefore, current study is only focus on the A-pillar part in which side view mirror part also will be included.

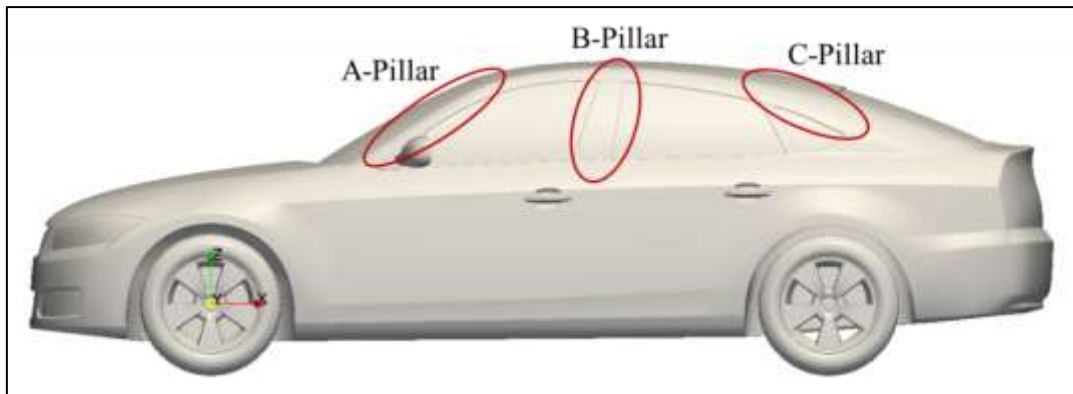


Figure 1.3 Three pillar configurations of DrivAer Fastback, a sedan-typed car model

## 1.2 Problem Statement

Due to the customers demand for a low level of cabin noise while at the same time keeping the cost of the car to a minimum, a study on the noise generation is needed in order to mitigate its noise source generation. At high speed, wind noise can dominates the total interior noise in which has caused discomfort for the passengers and the driver especially. Located near to the driver, A-pillar and side view mirror are the regions where the highly separated and turbulent flow are observed [14] and the relation and effects of the behaviour of flow over A-pillar and side view mirror on a realistic car are still not well understand.

The airflow around the A-pillar and side view mirror is very complex due to its turbulent nature and heavily governed by the unsteadiness behaviour of the fluids that thus contributes to the generation of wind noise at once [16] . Although, there are several studies on the wind noise generated by the flow over the A-pillar and side view mirror, there still a question on the reduction of noise level when the angle of A-pillar and length of side view mirror are varied on a real production car.

It is found that only several publications studied the wind noise associated with the flow from the A-pillar and side view mirror of a passenger car. Thus, the generation of wind noise over A-pillar and side view mirror is still not well understood especially

for the realistic production of car such as DrivAer model that would be used in this study. Nowadays, passenger comfort has becoming more important and therefore it is important to consider the automotive design in the early stage of process to make a reduction on noise for the car manufacturers as well as to cut the experimental cost and simultaneously improve its productivity and performance [17].

### **1.3 Research Objective**

The objectives of this research are :

- (a) To investigate the physical behaviour of wind generation on different slanted angle of the A-pillar and different length of the side view mirror of a realistic generic vehicle model called the DrivAer.
- (b) To analyze the most relevant slanted angle of the A-pillar of DrivAer that generates the lowest noise level.
- (c) To determine the best length of the side view mirror of DrivAer that produce the lowest level of wind noise.

### **1.4 Research Scope and Limitations**

The scopes of this research are as follows:

1. A realistic generic vehicle model, DrivAer is chosen as the problem geometry with the focused will be given on the wind noise generation on the A-pillar and side view mirror based on the flow characteristics.
2. The noise sources are primarily due to the pressure fluctuations and fluctuating aerodynamic forces which are drag, lift and side force.

3. The sound sources are considered as compact when the sound wavelength,  $\lambda$ , is larger than the dimension of the body,  $D$  ( $\lambda \gg D$ ).
4. Curle's equation is used in this study to calculate the noise radiation. In the Curle's equation, the noise generation due to pressure fluctuation on the surface of a rigid body is considered.
5. The research is only focused on the simulation method due to the complexity to separate the other noise sources from the wind noise in a real on road experiment.

This research is limited on noise generated from the A-pillar and side view mirror of symmetry body of the DrivAer model instead of a whole DrivAer body or other parts of car component such as the engine, radiator or tyres. The angle of A-pillar needs to follow the standard of its maximum and minimum of real production cars based on the standard for safety regulation as stated in Table 1.1 below. This is because the A-pillar angle and its width affect the structure of the rooftop of the production cars. Moreover, if the angle of the A-pillar is too small, the sunlight penetration would be directly to the driver and also to the front passenger.

Table 1.1 Standard European vehicles measurement regulations [18, 19, 20]

| <b>Measurement Description</b>                | <b>Mean</b>  | <b>Min</b> | <b>Max</b> |
|---|--|------------|------------|
| <b>A-pillar inclination from vertical (°)</b> | 57   | 40         | 61         |
| <b>Position of side view mirror (mm)</b>      | Must not projected more than 250 mm beyond the overall width of the vehicle measured without mirror. |            |            |



## 1.5 Significance of Research

Noise is not just unpleasant. It can be a major expense and productivity lost. With the increased speed of the vehicles, noise has become one of the environmental problems that need to be focused on. If this situation can be handled in a certain part, it would give a great impact on the driver and passenger while driving.

The study on wind noise radiated from the A-pillar and side view mirror of a realistic car can discover how much the level of noise propagated towards the driver. Reduction on noise level from A-pillar and side view mirror is expected to develop a comfort environment to the driver and passenger especially while driving at high speed and during a long journey. The study of wind noise generation based on the behaviour of flow that passing over the A-pillar and side view mirror may give the ideas to the designers and engineers to predict in advance their designed car at the early design stage.

Next, to signify the purpose of this study, studies about noise are not only understanding its propagation mechanism, but also to investigate the most effective method on controlling and reducing the noise. Based on the previous study, there are only several studies [14, 21–24] that systematically investigate the effects of changing the angle of the A-pillar and manipulating the length of side view mirror in order to mitigate its noise sources. However, the study only limited to simplified car model. With the current study, a more realistic car model is used, thus manufacturers able to focus on the best A-pillar angle and length of side view mirror that generate low level of noise.

The study would be beneficial due to the use of a realistic car model that able to explain a detailed flow structure around A-pillar and side view mirror that create noise, compared to a simplified car model such as SAE Type 4 model, used in most of the past studies. The realistic car model used in this study which is DrivAer, can provide a more reliable data or can be as a guideline for manufacturers on wind noise generation from the A-pillar and side view mirror.

## 1.6 Thesis Outline

This thesis is divided into six chapters. Chapter 1 provides basic introduction of the research by introducing the background of research, problem statement, the objectives of research, research scopes and limitations, and lastly the significance of research.

Chapter 2 discusses the literature review related to this study in detail including the review on the past studies which are important as a guideline for current study. Research gaps will be identified and highlighted based on the reviews.

Methodology for current study is explained in Chapter 3. It includes the methodology for flow simulation, noise calculation and sound transmission loss. Methods involved for flow simulation are the governing equations, turbulence model, wall function, problem geometry, computational domain, boundary conditions and computing machine. Method for noise calculation is explained starting from the basic acoustic analogy, followed by Lighthill's acoustic analogy, and finally the Curle's theory that is used in current study. Next, explanation for sound transmission loss method and finally the research flow is presented in a Gantt chart.

Chapter 4 describes the computational validation study for flow over DrivAer and the noise generated. This chapter is important in order to make sure that the method implemented in current study is correct and suitable for further progress by comparing the results from the validation case study with the previous available results. This includes the validation for flow simulation and noise calculation.

Chapter 5 presents the main findings of current study in which all the results obtained will be analysed and discussed. The results include the case of wind noise generated from both, the A-pillar and the side view mirror that are presented in the form of tables, graphs and flow visualisations.

Chapter 6 summarises the current study with conclusions and recommendation for future works.

## REFERENCES

- [1] Istvan L. Ver and Leo L. Beranek. *Noise and Vibration control.pdf*. Second Edi. Canada: John Wiley & Sons, Inc, 2006.
- [2] Chin C. Keeping That Noise Level Down. *Star Malaysia*. 31<sup>st</sup> July 2016. <https://www.thestar.com.my>
- [3] Mishra RK, Rangnekar S, Parida M. Survey on Noise Pollution and Its Management. *Journal of the IPHE, India* 2008; 2008-09: 30–34.
- [4] Ali MSM, Doolan CJ, Wheatley V. The sound generated by a square cylinder with a splitter plate at low Reynolds number. *J Sound Vib* 2011; 330: 3620–3635.
- [5] Samion SRL, Mat Ali MS, Abu A. Sound from high-Reynolds number flow over bluff bodies. *Aircr Eng Aerosp Technol* 2015; 87: 551–556.
- [6] Ono K, Himeno R, Fukushima T. Prediction of wind noise radiated from passenger cars and its evaluation based on auralization. *J Wind Eng Ind Aerodyn* 1999; 81: 403–419.
- [7] Ali MSM, Jalasabri J, Sood AM, et al. Wind noise from A-pillar and side view mirror of a realistic generic car model, DriAver. *Int J Veh Noise Vib* 2018; 14: 38.
- [8] Blokland GV, Peeters B. Modeling the noise emission of road vehicles and results of recent experiments. *Internoise 2009*.
- [9] Ali MSM, Jalasabri J, Sood AM, et al. Wind Noise From A-pillar and Side View Mirror of A Realistic Generic Car Model , DrivAer. *Int J Veh Noise Vib* 2018; 14: 38–61.
- [10] Lighthill MJ. On sound generated aerodynamically : II. Turbulence as a source of sound. *Proc R Soc A* 1954; 222: 1–32.
- [11] Hucho WH, Gino S. Aerodynamics of Road Vehicles. *Annu. Rev. Fluid Mech.* 1993; 25: 485-537.
- [12] Belamri T, Egorov Y, Menter F. CFD Simulation of the Aeroacoustic Noise Generated by A Generic Side View Car Mirror. *13th AIAA/CEAS Aeroacoustics Conf (28th AIAA Aeroacoustics Conf)* 2007; 1–12.
- [13] Franck G, D'Elia J. CFD modeling of the flow around the Ahmed vehicle

- model. *Proc 2nd Conf Adv Appl GiD* 2004; 5–8.
- [14] Hartmann M, Ocker J, Lemke T, et al. Wind Noise Caused by the Side-Mirror and A-Pillar of a Generic Vehicle Model. *18th AIAA/CEAS Aeroacoustics Conf (33rd AIAA Aeroacoustics Conf)* 2012; 4–6.
- [15] Heft A, Indinger T, Adams N. Investigation of Unsteady Flow Structures in the Wake of a Realistic Generic Car Model. *29th AIAA Appl Aerodyn Conf* 2011; 1–14.
- [16] Murad N, Naser J, Alam F, et al. Computational fluid dynamics study of vehicle A-pillar aero-acoustics. *Appl Acoust* 2013; 74: 882–896.
- [17] Nebenfuhr B. OpenFOAM : A tool for predicting automotive relevant flow fields. *Thesis* 2010; 1–114.
- [18] Quigley C. Field of vision ( A-pillar geometry ) - a review of the needs of drivers : final report. *Dept. of the Environment* 2001.
- [19] Parliament THEE, Council THE, The OF, et al. EU Mirror Law. *Official Journal of the European Union* 2003.
- [20] United N. Addendum 45: Regulation No. 46. Rev. 5 *Economic Commission for Europe*. 2013
- [21] Nouzawa T, Li Y, Kasaki N, et al. Mechanism of Aerodynamic Noise Generated from Front-Pillar and Door Mirror of Automobile. *J Environ Eng* 2011; 6: 615–626.
- [22] Buchheim R, Mankau DH, Schwabe D. Vehicle Interior Noise Related To External Aerodynamics. 1982; 3: 398–410.
- [23] Alam F. The Effects of Car A-pillar and Windshield Geometry on Local Flow and Noise. *Dept. of Mechanical and Manufacturing Eng.* 2000.
- [24] Heft AI, Indinger T, Adams NA. Experimental and Numerical Investigation of the DrivAer Model. *Proc ASME 2012 Fluids Eng Summer Meet* 2012; July 8-12: 1–11.
- [25] Doolan CJ. Computational bluff body aerodynamic noise prediction using a statistical approach. *Appl Acoust* 2010; 71: 1194–1203.
- [26] Choi H, Jeon WP, Kim J. Control of flow over a bluff body. *Annu Rev Fluid Mech* 2008; 40: 113–139.
- [27] Ali MSM. Flow and noise associated with the interaction of a square cylinder with a downstream flat plate. *School of Mech. Eng.* 2011; 1–245.
- [28] Choi CK, Kwon DK. Determination of the Strouhal number based on the

- aerodynamic behavior of rectangular cylinders. *Wind Struct An Int J* 2000; 3: 209–220.
- [29] Tsubokura M, Kobayashi T, Nakashima T, et al. Computational visualization of unsteady flow around vehicles using high performance computing. *Comput Fluids* 2009; 38: 981–990.
- [30] White FM. *Viscous Fluid Flow*, Third Edition. *McGrawHill* 2006; 1-629.
- [31] Bearman P. Bluff body flows applicable to vehicle aerodynamics. *Journal of Fluids Eng.* 1980; 102: 265-274
- [32] Hucho WH. *Aerodynamics of Road Vehicles*. 4th Edition. *SAE Publication*. 1998.
- [33] Buchheim R, Mankau DH, Schwabe D. Vehicle Interior Noise Related To External Aerodynamics. *Int J Veh Des* 1982; 3: 398–410.
- [34] George AR, Callister JR. Aeroacoustics of passenger cars-State-of-the-art. In: *Seminar Aerodynamics and powertrain alltomobile noise-Aeroacollstics*. 1996.
- [35] Barnard RH. *Road vehicle aerodynamic design: an introduction*. Longman, 1996.
- [36] Zimmer G, Alam F, Watkins S. The contribution of the A-Pillar vortex to passenger car in-cabin noise. *Proc 4th Aust Fluid Mech Conf* 2001; 111–114.
- [37] Jakirlic S, Kutej L, Basara B, et al. Computational Study of the Aerodynamics of a Realistic Car Model by Means of RANS and Hybrid RANS/LES Approaches. *SAE Int J Passeng Cars - Mech Syst* 2014; 7: 559-574.
- [38] Katz J. *Race Car Aerodynamics* 1st Edition. *Bentley Publisher*. 1995.
- [39] Hammond C, Wade MG. Forward looking blindspots: A report of A-pillar induced field-of-view obstruction and driver performance in a simulated rural environment. *Adv Transp Stud* 2005; 69–81.
- [40] Krajnović S, Östh J, Basara B. LES study of breakdown control of A-pillar vortex. *Int J Flow Control* 2010; 2: 237–258.
- [41] Dechpre H, Hartmann M. Aeroacoustics Simulation of an Automotive A-Pillar Rain Gutter. *Eur Automot Simul Conf Aeroacoustics* 2009; 1–12.
- [42] Popat BC. Study of flow and noise generation from car A-pillars. *Univ. of London*. 1991.
- [43] Hoarau C, Borée J, Laumonier J, et al. Unsteady wall pressure field of a model A-pillar conical vortex. *Int J Heat Fluid Flow* 2008; 29: 812–819.
- [44] Watanabe M, Harita M, Hayashi E. The Effect of Body Shapes on Wind Noise.

- SAE Tech Pap Ser.* 1978.
- [45] He Y, Shi Z, Wu Y, et al. Sound Radiation Analysis of a Front Side Window Glass of DrivAer Model under Wind Excitation. *Shock and Vibration* 2018.
  - [46] He Y, Schröder S, Shi Z, et al. Wind noise source filtering and transmission study through a side glass of DrivAer model. *Appl Acoust* 2020; 160: 107161.
  - [47] Stapleford WR, Carr GW. Aerodynamic noise in road vehicles, part 1: The relationship between aerodynamic noise and the nature of the airflow. *Mot Ind Res Assoc* 1970.
  - [48] Sadakata O, Kanamaru K, Kakamu T. A Consideration Of Wind Noise Reduction by Air Flow Control. *SAE Tech Paper.* 2010.
  - [49] Haruna S, Kamimoto I, Okamoto S. Estimation Method for Automobile Aerodynamic Noise. *SAE Tech Paper.* 2010.
  - [50] Hanaoka Y, Zhu M, Miyata H. Numerical Prediction of Wind Noise Around the Front Pillar of a Car-Like Body. *SAE Tech Paper.* 2010.
  - [51] Murad N, Naser J, Alam F, et al. Computational aero-acoustics of vehicle a-pillar at various windshield radii. *5th Int Conf CFD Process Ind* 2006; 1–6.
  - [52] Shojaefard MH, Goudarzi K, Fotouhi H. Numerical study of airflow around vehicle A-pillar region and windnoise generation prediction. *Am J Appl Sci* 2009; 6: 276–284.
  - [53] He Y, Wan R, Liu Y, et al. Transmission characteristics and mechanism study of hydrodynamic and acoustic pressure through a side window of DrivAer model based on modal analytical approach. *J Sound Vib* 2021; 501: 116058.
  - [54] Okutsu Y, Hamamoto N, Yanagimoto K, et al. Verification of Automobile Aerodynamic Noise Transmitted through Side Window Glass. *J Environ Eng* 2013; 8: 41–56.
  - [55] Freed D, Mutnuri LAR, Powell R, et al. Computational Process for Wind Noise Evaluation of Rear-View Mirror Design in Cars. *SAE Tech Paper* 2014; 1: 1–6.
  - [56] Roditcheva O. Experimental and Numerical Study of Wind Noise Caused by Cowl Area on Volvo XC60. *15th Stuttgart Int Symp* 2015; 1: 471–484.
  - [57] Becker S, Nusser K, Oswald M. Aero-Vibro-Acoustic Wind Noise-Simulation Based on the Flow around a Car. *SAE Tech Paper.* 2016.
  - [58] Phan VL, Wakamatsu M, Yasuki T, et al. A CFD Analysis Method for Prediction of Vehicle Exterior Wind Noise. *SAE Int J Passeng Cars - Mech Syst* 2017; 10: 286–298.

- [59] Viegas KR, Mukkamala Y. Detail optimization of the tesla model S to alleviate aero-acoustic noise and increase range. *Int J Appl Eng Res* 2016; 11: 6361–6372.
- [60] Mutnuri LAR, Senthoooran S, Powell R, et al. Computational Process for Wind Noise Evaluation of Rear-View Mirror Design in Cars. *SAE Tech Paper* 2014; 1: 1–6.
- [61] Menter FR, Kuntz M, Langtry R. Ten Years of Industrial Experience with the SST Turbulence Model. *Turbulence, Heat and Mass Transfer* 4. 2003.
- [62] Boussinesq J. Essay on Theory of Running Water. *Imprimerie nationale*. 1877.
- [63] Wilcox DC. Comparison of two-equation turbulence models for boundary layers with pressure gradient. *AIAA J* 1993; 31: 1414–1421.
- [64] Menter FR. Two-Equation Eddy Viscosity Turbulence Models for Engineering Applications. *AIAA Journal*. 1994; 32:1598-1606.
- [65] Shih TH, Povinelli LA, Liu NS. Application of Generalized Wall Function for Complex Turbulent Flows. *Elsevier Ltd*. 2002.
- [66] Versteeg HK, Malalasekera W. An introduction to computational fluid dynamics: the finite volume method. *Pearson education*, 2007.
- [67] Shih TH, Povinelli LA, Liu NS. Application of Generalized Wall Function for Complex Turbulent Flows. *Elsevier Ltd*, 2002.
- [68] Ahmend H, Chacko S. Computational Optimization of Vehicle Aerodynamics. *Symp Int Daaam* 2012; 23: 313–318.
- [69] Islam M, Decker F, Hartmann M, et al. Investigations of Sunroof Buffeting in an Idealised Generic Vehicle Model - Part I: Experimental Results. *14th AIAA/CEAS Aeroacoustics Conf (29th AIAA Aeroacoustics Conf)* 2008; 2900: 5–7.
- [70] Ahmed SR, Ramm G, Faltin G. Some Salient Features of The Time-Averaged Ground Vehicle Wake. *SAE Tech Paper*. 1984.
- [71] Soares RF, Souza FJ De. Investigation of Cfd Setup for Automotive Applications. *POSMEC*. 2014; 26–29.
- [72] Ringwall E. Aeroacoustic sound sources around the wheels of a passenger car A Computational Fluid Dynamics study using steady state models to evaluate main sources of flow noise Master’s thesis in Applied Mechanics. *Chalmers University of Tech*. 2017.
- [73] Soares R, de Souza F. Proposal of an Aerodynamic Concept for Drag Reduction

- of Fastback Car Models. *SAE Tech Paper*. 2014; 2009:26–29.
- [74] Shaharuddin NH, Mat Ali MS, Mansor S, et al. Numerical Study For Flow Over A Realistic Generic Model, DrivAer, Using URANS. *J Adv Res Fluid Mech Therm Sci* 2018; 48: 183–195.
- [75] Heft AI, Indinger T, Adams NA. Introduction of a New Realistic Generic Car Model for Aerodynamic Investigations. *SAE International*. 2012.
- [76] Norton MP, Karczub DG. Fundamentals of noise and vibration analysis for engineers. *Cambridge university press*. 2003.
- [77] Oettle N, Sims-Williams D. Automotive aeroacoustics: An overview. *Proc Inst Mech Eng Part D J Automob Eng* 2017; 231: 1177–1189.
- [78] Uosukainen S. Foundations of acoustic analogies. *VTT Publications*. 2011; 757:1-121.
- [79] Leong S. Noise pollution concerns for the MRT Project (Part 2). *Free Malaysia Today*. 14<sup>th</sup> Dec2011. <http://www.freemalaysiatoday.com/>.
- [80] Curle N. The influence of solid boundaries upon aerodynamic sound. *Proc R Soc A* 1955; 231: 505–514.
- [81] Lighthill MJ. On sound generated aerodynamically : I. General theory. *Proc R Soc A* 1951; 211: 564–587.
- [82] Friman M. Directivity of sound from wind turbines. *Dept. of Aeronautical and Vehicle Engineering*. 2011; 42.
- [83] Cooley JW, Lewis PAW, Welch PD. The Fast Fourier Transform and its Applications. *IEEE Trans Educ*. 1969; 12: 27–34.
- [84] Ali MSM, Shaharuddin NH, Jalasabri J, et al. Validation Study on External Wind Noise Prediction using OpenFOAM. *J Mech Eng* 2018; 7: 111–126.
- [85] Ishak IA, Ali MSM, Shaikh Salim SAZ. Mesh size refining for a simulation of flow around a generic train model. *Wind Struct An Int J* 2017; 24: 223–247.
- [86] Shaharuddin NH, Ali MSM, Mansor S, et al. Numerical study for flow over a realistic generic model, DrivAer, using URANS. *J Adv Res Fluid Mech Therm Sci* 2018; 48: 183–195.
- [87] Lizarose SR, Shaharuddin NH, Mat Ali MS. Grid Convergence Study for Detached-Eddy Simulation of Flow over Rod-Airfoil Configuration Using OpenFOAM. *IOP Conf Ser Mater Sci Eng*. 2019.
- [88] Maruai NM, Ali MSM, Ismail MH, et al. Flow-induced vibration of a square cylinder and downstream flat plate associated with micro-scale energy



- harvester. *J Wind Eng Ind Aerodyn* 2018; 175: 264–282.
- [89] Celik I, Ghia U, Roache PJ, et al. Procedure for Estimation and Reporting of Uncertainty Due to Discretization in CFD Applications. *J Fluids Eng.* 2008; 130: 078001.
- [90] Richardson LF, Gaunt JA. The Deferred Approach to the Limit. Part I. Single Lattice. Part II. Interpenetrating Lattices. *Philos Trans R Soc London Ser A, Contain Pap a Math or Phys Character.* 1927; 226: 299–361.
- [91] Roache PJ. Perspective: A Method for Uniform Reporting of Grid Refinement Studies. *J Fluids Eng.* 1994; 116: 405–413.
- [92] Stern F, Wilson R V, Coleman HW, et al. Code Verification of unsteady flow solvers with method of manufactured solutions. *Int J Offshore Polar Eng.* 2008; 18: 120–126.
- [93] Ali MSM, Doolan CJ, Wheatley V. Grid Convergence Study for a Two-Dimensional Simulation of Flow Around a Square Cylinder At a Low Reynolds Number. *Seventh Int Conf CFD Miner Process Ind CSIRO.* 2009; 1–6.
- [94] Wilcox DA. Simulation of Transition with a Two-Equation Turbulence Model. *AIAA Journal.* 1994; 32: 247–255.
- [95] Guilmineau E. Numerical Simulations of Flow around a Realistic Generic Car Model. *SAE Int J Passeng Cars - Mech Syst.* 2014; 7: 2014-01–0607.
- [96] Shinde G, Joshi A, Kishor N. Numerical Investigations of the DrivAer Car Model using Opensource CFD Solver OpenFOAM Numerical Investigations of the DrivAer Car Model using Opensource CFD Solver OpenFOAM Abstract : In: *Tata Consultancy Services, Pune, India.* 2016, pp. 0–12.
- [97] Ashton N, West A, Lardeau S, et al. Assessment of RANS and DES methods for realistic automotive models. *Comput Fluids.* 2016; 128: 1–15.
- [98] Rüttgers M, Park J, You D. Large-eddy simulation of turbulent flow over the DrivAer fastback vehicle model. *J Wind Eng Ind Aerodyn.* 2019; 186: 123–138.
- [99] Aljure DE, Calafell J, Baez A, et al. Flow over a realistic car model: Wall modeled large eddy simulations assessment and unsteady effects. *J Wind Eng Ind Aerodyn.* 2018; 174: 225–240.
- [100] Samion SRL. The Effect of Crosswind on Aeolian Tone Generation for Rectangular Prisms Arranged in Tandem. *Universiti Teknologi Malaysia.* 2017.
- [101] Na Y, Moin P. The structure of wall-pressure fluctuations in turbulent boundary layers with adverse pressure gradient and separation. *J Fluid Mech.* 1998; 377:

347–373.

- [102] Kim J, Sung HJ. Wall pressure fluctuations and flow-induced noise in a turbulent boundary layer over a bump. *J Fluid Mech.* 2006; 558: 79.
- [103] Cho M, Kim HG, Oh C, et al. Benchmark study of numerical solvers for the prediction of interior noise transmission excited by A-pillar vortex. *Internoise 2014* 2014; 1–10.
- [104] Murad NM, Naser J, Alam F, et al. Simulation of Vehicle A-Pillar Aerodynamics of Various Yaw Angles. *15<sup>th</sup> Australasian FLuid Mech. Conf.* 2004; 13: 17.
- [105] Soares RF, Souza FJ De. Influence of numerics and analysis of external flow over a three-dimensional realistic car model. *Turbulence, Heat and Mass Transfer* 8. 2015; 2009: 8–11.
- [106] Howell J, Fuller JB, Passmore M. The effect of free stream turbulence on A-pillar airflow. *SAE Technical Paper.* 2009.